

Problems of Predicting Turbulent Burning Rates

Derek Bradley
School of Mechanical Engineering, University of Leeds
Leeds LS2 9JT, UK
d.bradley@leeds.ac.uk

Introduction

At present there are two main approaches to the understanding and mathematical modelling of practical turbulent combustion. These involve the joint probability density function (JPDF) transport equations [1,2] and laminar flamelets [3,4]. There is no conflict in the way the complexities of turbulent-reaction interactions are handled, but each approach emphasises different aspects and the computational requirements are different. The JPDF approach is capable of exactly representing the interaction of chemical reactions and convection, although viscous dissipation and turbulent mixing of scalars must be closed by modelling. The computational demands of detailed chemistry can be excessive, but these diminish with intrinsic low-dimensional manifolds (ILDm) [5] that reduce the chemistry from that of a fully detailed scheme. The *in situ* adaptive tabulation, ISAT, algorithm [6] also reduces the computational effort.

Direct numerical simulations (DNS) [7] are valuable in suggesting closure procedures in moment methods, while large eddy simulations (LES) [8] give a more realistic picture of practical flows than do first and second moment models. Laminar flamelet methods computationally uncouple the chemistry from the turbulence in stretched laminar flame studies then re-couple it in the turbulent flame. The conditional moment closure (CMC) approach [9] has affinities with flamelet methods. With CMC in non-premixtures most of the scalar fluctuation can be associated with the mixture fraction, and conditional averaging with respect to it allows closure of the conditional average chemical reaction term. Normally these conditional fluctuations of the reactive scalars are smaller than the unconditional fluctuations and can be neglected. If they are not, conditioning of second moments might be employed.

The laminar flamelet approach has proved rather more robust and effective than might originally have been anticipated. One reason, revealed by direct numerical simulations, is that a continuous laminar flame structure can be thickened by small scale turbulence without invalidating the flamelet assumption [7,10]. As a result, a Karlovitz flame stretch factor can be accommodated which is 17 times that of the Klimov-Williams limit [11].

The principal parameters that express burning rate are the turbulent burning velocity and the mean volumetric heat release rate. The burning velocity is rather difficult either to define precisely or to measure rigorously. It is not a convenient parameter when there is no readily discernible propagating flame front, as in furnaces and gas turbine combustion chambers with recirculating flow, or when the front is severely disrupted at high Karlovitz stretch factors. Under such conditions, the mean volumetric heat release rate is a more convenient parameter and computation of its spatial distribution can be readily incorporated into CFD codes.

The paper attempts a unified approach, that embraces both of these parameters, and highlights some current problems. A new expression is presented for the turbulent burning velocity, based on a universal pdf of turbulent strain rates, with both flamelet burning and quenching controlled by Markstein numbers, and some fractal considerations. Different expressions for the turbulent burning velocity are compared.

Mean volumetric heat release rate

In turbulent premixed flames the mean volumetric heat release rate, \bar{q}_t can be expressed in terms of that in stretched laminar flamelets $q_\ell(\theta, s)$ by [12]:

$$\bar{q}_t = \int_{s_{q-}}^{s_{q+}} \int q_\ell(\theta, s) p(\theta, s) d\theta ds \quad (1)$$

Here s_{q+} and s_{q-} are flame extinction stretch rates under positive and negative strain rates. Numerical analyses of laminar flames, with detailed kinetics, suggest the volumetric heat release rate, $q_\ell(\theta, s)$ at a dimensionless temperature rise, θ , and a stretch rate, s , is simply related to that at zero stretch rate, $q_{\ell 0}(\theta)$, by [12]:

$$q_\ell(\theta, s) = f(s) q_{\ell 0}(\theta) \quad (2)$$

where $f(s)$ is a function that depends upon s and the Markstein numbers of the mixture. If the influences of θ and s are assumed to be uncorrelated, the joint pdf, $p(\theta, s)$, may be expressed by the product of the two separate pdfs, $p(\theta)p(s)$ and

$$\bar{q}_t = P_b \int_0^1 q_{\ell 0}(\theta) p(\theta) d\theta \quad (3)$$

with flame stretch rate effects grouped together in a ‘‘probability of burning’’ factor, P_b :

$$P_b = \int_{s_{q-}}^{s_{q+}} f(s) p(s) ds \quad (4)$$

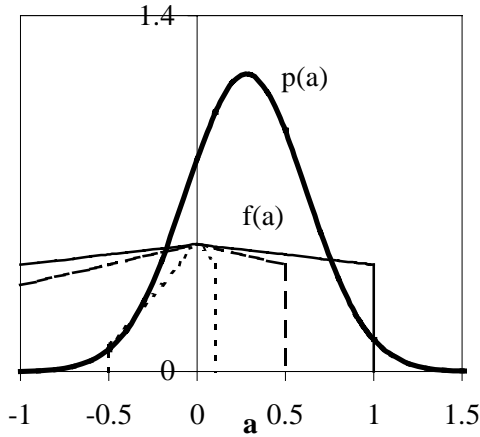


Figure 1(a). $L_{sr} \geq 0$

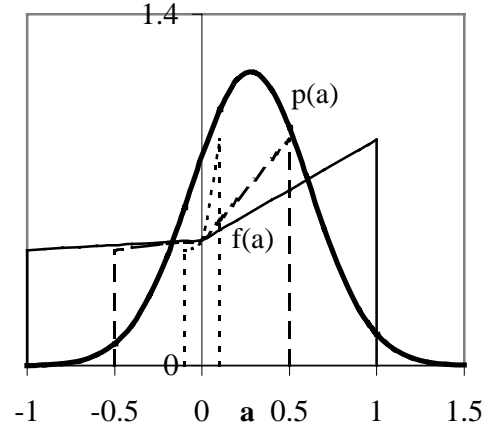


Figure 1(b). $L_{sr} \leq 0$

Values of $f(a)$ half scale. Full lines $\tau_\eta = 1$ ms, dashed lines $\tau_\eta = 0.5$ ms, dotted lines $\tau_\eta = 0.1$ ms.

The forms of the pdfs $p(\theta)$ and $p(s)$ are assumed *a priori* and evaluated from computed first and second moments of assumed pdfs in a CFD system of equations, including first and second moment energy equations and Reynolds stress modelling [11,13]. That for θ assumes a beta function and that for s follows the direct numerical simulations of Yeung et al. [14], albeit for a low turbulent Reynolds number. The strain rate, s , is normalised by multiplying it by the Kolmogorov time, τ_η , to give a dimensionless strain rate, a . This near-gaussian form of $p(a)$ for a material surface is shown in Fig. 1. The mean value of the dimensionless strain rate is 0.279 (corresponding to $1.08u'/\lambda$, where u' is the rms turbulent velocity and λ is the Taylor microscale) and the dimensionless rms

strain rate is 0.34. Studies of spherically propagating laminar flames of methane and propane mixtures over ranges of equivalence ratios, ϕ , have shown [12] that empirically $f(s)$ is given by:

$$f(s) = 1 - 0.8 \frac{L_{sr}s}{u_\ell} \quad \text{for } L_{sr}s \geq 0 \quad (5)$$

and

$$f(s) = 1 - 0.8 \frac{L_s s}{u_\ell} \quad \text{for } L_s s \leq 0$$

Without the factor of 0.8 these expressions are the same as those for u_{nr}/u_ℓ and u_n/u_ℓ , respectively [15]. Here u_ℓ is the unstretched laminar burning velocity, u_n the stretched laminar burning velocity based on the rate of entrainment of cold gas and u_{nr} that based on the rate of production of burned gas, with L_{sr} and L_s the associated Markstein lengths.

Equation (5) is expressed in terms of α by

$$f(a) = 1 - 0.8 \frac{L_{sr}a}{u_\ell \tau_\eta} \quad \text{and} \quad f(a) = 1 - 0.8 \frac{L_s a}{u_\ell \tau_\eta}, \quad \text{respectively.} \quad (6)$$

Quench is indicated by sudden decreases of $f(s)$ and $f(\alpha)$ to zero at $s = s_{q+}$ and s_{q-} ($a = a_{q+}$ and a_{q-}). Figure 1 illustrates the influence of increasing turbulence as τ_η is reduced from 1 to 0.5 and 0.1 ms, for $u_\ell = 1$ m/s and $s_{q+} = 1000$ s⁻¹. The influence of negative flame stretch is difficult to assess, because flames stretched in this way are inherently unstable and difficult to study. The approach in [12] is therefore adopted. This extrapolates the value of u_n to zero at negative s to yield $s_{q-} = u_\ell/L_s$. The values of $f(a)$ plotted in Fig. 1(a) are for $L_{sr} = 0.2$ mm, and $L_s = -0.2$ mm. Those in Fig. 1 (b) are for $L_{sr} = -0.1$ mm, and $L_s = -1$ mm. As the turbulence increases $p(\alpha)$ is assumed to be unchanged, but the associated decreases in τ_η narrow the limits between a_{q+} and a_{q-} . Because $s_{q+} = 1000$ s⁻¹, for $\tau_\eta = 1, 0.5,$ and 0.1 ms, values of a_{q+} have the same numerical values as τ_η in ms. For values of α greater than these and less than a_{q-} there is no flame propagation.

Equation (4) becomes $P_b = \int_{a_{q-}}^{a_{q+}} f(a)p(a)da$ and reference to Fig. 1(a) shows that as the turbulence increases, the proportion of the spectrum of strain rates capable of sustaining combustion decreases, along with P_b . This principally results from the decrease in a_{q+} and increase in a_{q-} , but with some contribution from the positive value of L_{sr} . The corresponding Markstein number, Ma_{sr} , is L_{sr}/δ_ℓ , where the flame thickness, δ_ℓ , is given by ν/u_ℓ and ν is the kinematic viscosity. The situation is different in Fig. 1 (b) where the negative values of L_{sr} and Ma_{sr} result in higher values of P_b . As τ_η decreases from very large values, at which there is negligible flame quenching, P_b can at first increase. With further increase, flame quenching becomes dominant and P_b decreases.

Turbulent burning velocity

Heat release rate in the source term

The analyses of flame leading edges in [16-19] show the turbulent burning velocity for given turbulent parameters to be proportional to $\bar{q}_t^{0.5}$. It is convenient also to postulate a turbulent flame

with a turbulent burning velocity, u_{to} , and mean heat release rate, \bar{q}_{to} , for the same turbulent parameters, but for which fluctuations in strain rates and reaction progress variable, θ , influence neither u_ℓ nor the mean heat release rate of flamelets, with $f(a)=1$. Nor is there any flame quenching. This implies a corresponding value of $P_b = \int_{-\infty}^{+\infty} p(a)da$, of unity and hence, with Eqs. (3) and (4):

$$\frac{u_t}{u_{to}} = \left(\frac{\bar{q}_t}{\bar{q}_{to}} \right)^{0.5} = \left(\frac{P_b \int_0^1 q_{\ell o}(\theta) p(\theta) d\theta}{\int_{-\infty}^{+\infty} p(a) da \int_0^1 q_{\ell 0}(\theta) p(\theta) d\theta} \right)^{0.5} = P_b^{0.5} \quad (7)$$

The value of u_{to} can be obtained from fractal considerations. With an outer cut-off equal to the integral length scale of turbulence, l , and an inner cut-off equal to the Gibson scale, l_G , the mean surface area ratio, σ , of the fractal surface with l_G as the inner cut-off to that with l as the outer cut-off is [20]:

$$\sigma = \left(\frac{l}{l_G} \right)^{D-2} = F \frac{u'}{u_\ell} \quad \text{where} \quad F = \frac{2\pi^{2/3} C^{1/3} (1.5)^{0.5}}{C_K} \quad (8)$$

With the fractal dimension, $D = 7/3$, the Kolmogorov constant, $C_K = 1.7$, the ratio $l/\lambda = 0.25R_l^{0.5}$ (R_l is the turbulent Reynolds number based on l) and a consequent value of $C_D = 0.51$, then $F = 2.0$. Uncertainties in the value of C_K mean the accuracy of F is no better than two significant figures.

With no flame stretch or quench to influence the wrinkled flame area [20] the surface area ratio in Eq. (8) must give a burning velocity ratio due to surface wrinkling. This is usually equated to u_{to}/u_ℓ , although it is a slight overestimate, due to the wrinkling at the outer cut-off. Experimental data [21] suggests that as $u'/u_\ell \rightarrow 0$, $u_{to}/u_\ell \rightarrow 1$, not 0, as suggested by Eq. (8). Hence, following Gulder [22], though for a different inner cut-off, we take:

$$\frac{u_{to}}{u_\ell} - 1 = F \frac{u'}{u_\ell} \quad (9)$$

The experimental data in [21] suggest this is valid for $u'/u_\ell \geq 1$. Hence, from Eqs. (7) and (9):

$$\frac{u_t}{u'} = U = \left(\frac{u_\ell}{u'} + F \right) P_b^{0.5} \quad \text{for } u_\ell/u' \leq 1.0 \quad (10)$$

In [12] it is postulated that extinction of a laminar flame under a positive strain rate occurs when the preheat and reaction zones have become so swollen with unburned gas that reaction can no longer be sustained. A criterion is developed for this, in terms of the difference $(Ma_{sr} - Ma_s)$. Along with Eqs. (1) to (5), this enables values of P_b to be obtained as a function of Ma_{sr} , Ma_s and the Karlovitz stretch factor, K , $(u'/\lambda)(\delta_\ell/u_\ell)$. Here, the value of K is based on $l/\lambda = 0.25R_l^{0.5}$ and consequently $K = 0.25(u'/u_\ell)^2 R_l^{-0.5}$. In [23] values of u_t in explosion flames have been carefully measured using Mie scattering from planar sheets. For $Ma_{sr} \geq 1.0$ and with values of P_b from [12] these yield a mean value of F of 2.2, while the flamelet CFD model in [13] yields $F = 2.45$ for methane-air mixtures. A value of $F = 2.3$ therefore was selected to evaluate U from Eq. (10).

Values of U , with u_ℓ/u' assumed to be negligibly small, are shown plotted against $K(Ma_{sr} - Ma_s)$ in Fig. 2 for atmospheric flames with different values of Ma_{sr} . The bold, full line curve covers atmospheric propane-air, ϕ 0.7 to 1.0, and near-stoichiometric methane-air mixtures, with values of Ma_{sr} ranging from 3.9 to 6.2. The broken curves are for propane-air: the dashed curve for $\phi = 1.3$ ($Ma_{sr}=1.29$) and the dotted curve for $\phi = 1.4$ ($Ma_{sr}=-0.08$). As Ma_{sr} decreases and eventually becomes negative the ratio U increases significantly, as is shown clearly for $\phi = 1.4$. The approach outlined in this section allows for the influence of stretch rate on flame propagation and ultimately extinction, using only the physicochemical parameters of u_ℓ , Ma_{sr} and Ma_s . The influence of Markstein numbers is clearly important. For example, for a propane mixture, $\phi = 1.3$, $u_\ell = 0.32$ m/s and with $K = 0.2$, then $U = 1.4$, but for the corresponding lean mixture with the same values of u_ℓ and K then $U = 1.0$. For the same turbulence the rich mixture has a value of u_t that is 40% higher.

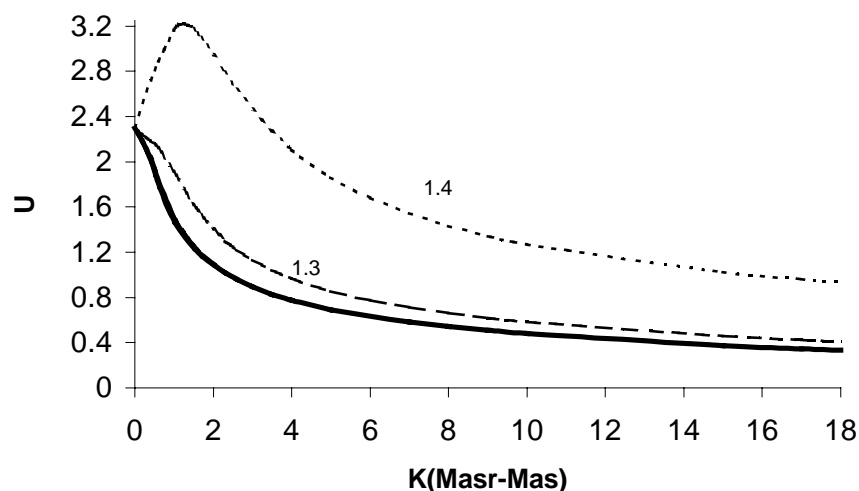


Figure 2. Variation of U from Eq. (10) with $K(Ma_{sr} - Ma_s)$ for different ϕ for propane-air.

Laminar burning velocity in the source term

In flamelet models that involve the flame surface density, Σ , the source term is of the form $\rho_u u_\ell I_o \Sigma$, where ρ_u is the density of the reactants and I_o is a flame stretch factor [19]. Transport equations have been formulated for Σ [24] and some of the predictions of u_t from these are compared with experimental values in [25].

The G equation [26] presents an alternative flame surface approach to premixed combustion. The non-reacting scalar, G , is defined at the flame surface and the propagation of the flame sheet is expressed by:

$$\frac{\partial G}{\partial t} + v \cdot \nabla G = u_n |\nabla G| \quad (11)$$

The localised burning velocity normal to the flame front is u_n , and v is the flow velocity. When combined with the global mass conservation equation, Eq. (11) takes on the more familiar, computationally advantageous, conservation form. Peters [27] has assumed the validity of the G

equation for the entire flow field and split G and v into Favre mean and variance equations. From scaling arguments, a model equation for the mean flame surface area ratio, $\bar{\sigma}_t$, the increase in flame surface area caused by turbulence, is derived. To this is added the laminar contribution. This equation has similarities with the Σ equation [24]. The solution of the $\bar{\sigma}_t$ equation, with the substitution of the recommended values of two modelling constants [28] yields:

$$U = \frac{u_\ell}{u'} + \frac{0.39Da}{b_1} \left[\left(1 + \frac{5.13b_1^2}{Da} \right)^{1/2} - 1 \right] \quad (12)$$

Here Da is the Damköhler number, $= u_\ell l / u' \delta_\ell$, and $K = 0.25(u' / u_\ell) Da^{-0.5}$. In [28] the constant b_1 , is taken to be 2. This constant is essentially the same as F in the present study. As Da and $u' / u_\ell \rightarrow \infty$ in the large scale turbulence regime, $U \rightarrow b_1$, just as in Eq. (10), as K and $u_\ell / u' \rightarrow 0$, $U \rightarrow F$. Damköhler's small scale turbulence regime is approached as $D \rightarrow 0$. Flame stretch, Lewis, Le , and Markstein number effects do not enter into this model.

Equation (11) was also a starting point for Yakhot in his application of renormalisation group (RNG) methods to obtain an expression for u_t / u_ℓ [29]. The flame surface is wrinkled by the cascade of turbulent energy that terminates at the Kolmogorov scale and the RNG methodology effectively averages over gradually increasing scales, while the fluid motion is governed by the Navier-Stokes equation. No allowance is made for thermo-diffusive effects and the analysis yields:

$$U = \frac{u_\ell}{u'} \exp(U)^{-2} \quad (13)$$

In attempts to provide better agreement with experiment, extension of the model to include the effects of scales smaller than δ_ℓ resulted in predictions closer to experiment [30]. Sivashinsky [31] in a related approach, but with a series of discrete waves, pointed to the inhibiting effect of flame stretch which may lead to extinction.

An extensive correlation of 1650 measurements of u_t , over a wide range of K and Le was presented in [21]. With the present expression for l / λ it gives:

$$U = 1.01(KLe)^{-0.3} \text{ for } 0.02 \leq KLe \leq 1.0 \quad (14)$$

Klimenko [32] has employed the cascade hypothesis, but with fewer theoretical modelling assumptions and with scaling factors determined from the experimental data of [21]. This enabled account to be taken of K and Le , and Eq. (14) to be recovered. At high KLe localised quenching becomes extensive in regions with high dissipation rates, the flame becomes fragmented and no longer presents a continuous surface. Large scale fluctuations can no longer stretch the flame front, the fractal dimension decreases, most of the wrinkling occurs at the smallest scales and R_l exerts a decreasing influence.

Another correlation of measured values of u_t / u_ℓ in the wrinkled flame regime by Gülder [33] gives:

$$U = \frac{u_\ell}{u'} + 0.62 \left(\frac{u_\ell}{u'} \right)^{0.5} R_l^{0.25} \quad (15)$$

Values of turbulent burning velocity compared

Predictions from the different expressions are compared in plots of U against $K(Ma_{sr} - Ma_s)$ in Fig. 3. Each curve is labelled by the corresponding equation number. A broken curve is for $R_l = 100$ and

a full one is for $R_l = 1000$. Only Eqs. (10) and (14) take account of thermo-diffusive effects. A common datum therefore is necessary for the comparison and this is provided by taking values of Le , Ma_{sr} and Ma_s , of 1.05, 3.85 and -4.57 , respectively, appropriate to stoichiometric methane-air under atmospheric conditions [15]. In all equations, save Eq. (14), u_ℓ/u' is evaluated from

$$u_\ell/u' = \left(0.25/(KR_l^{0.5})\right)^{0.5}.$$

At higher values of $K(Ma_{sr} - Ma_s)$ than those presented flames become disrupted by localised quenching and it is difficult to measure u_t . The two correlations of measured values, (14) and (15), are fairly close to each other. All correlations follow the same trend, with U decreasing as K increases, although (13) seems to under-estimate U appreciably. Otherwise, the biggest discrepancy is between (10) and (12), probably due to the neglect of flame stretch in the latter. The discrepancy would be greater were both expressions to employ the same values for F and b_1 . Because (10) is based on an overall mean reaction rate, in the form of \bar{q}_t , it probably expresses a burning velocity related to the rate of production of burned gas, whereas (12) and some of the experimental measurements are more likely to be based on the entrainment of cold gas, which gives a higher turbulent burning velocity [23]. This discrepancy between the two values of burning velocity is well known and has been shown to increase with K [34].

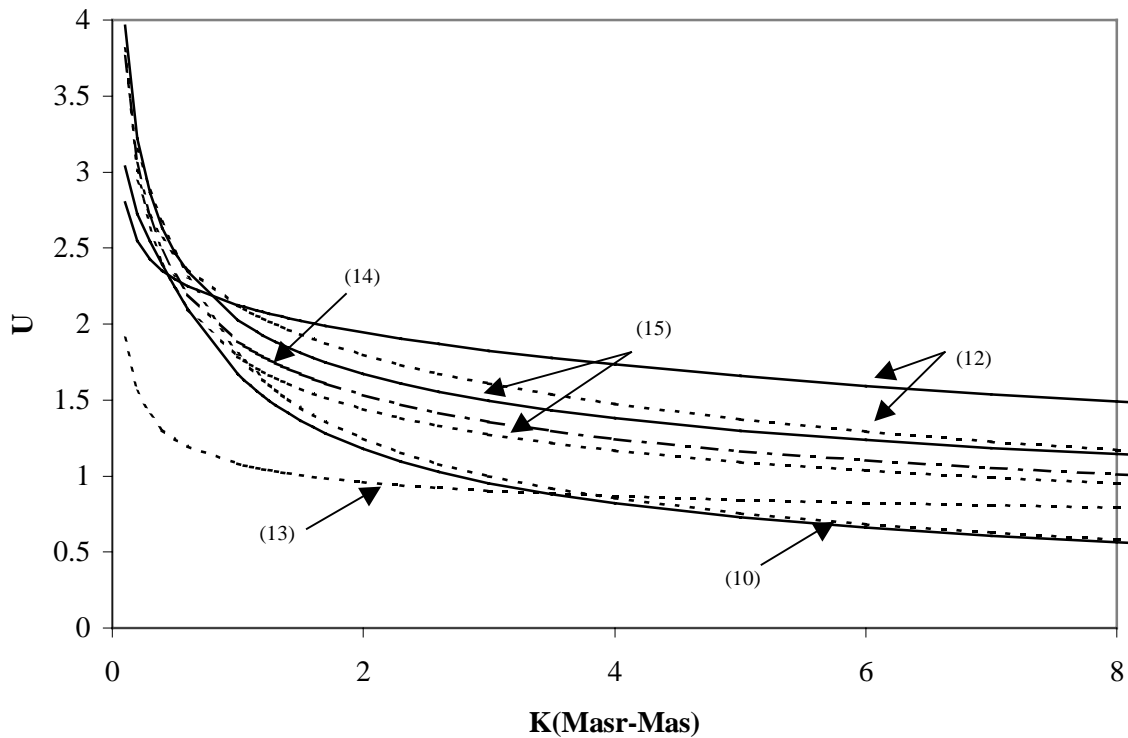


Figure 3. Variations of U for different equations. Dotted lines $R_l = 100$, full lines $R_l = 1000$.

Unstable laminar flames

The limit $K \rightarrow 0$ is of interest because it covers the transition regime between laminar and turbulent combustion. For a laminar flame, a combination of low stretch and low Ma_{sr} leads to flame instabilities that wrinkle the flame and consequently increase the overall burning velocity [35,36].

The Karlovitz stretch factor, K , essentially expresses a dimensionless flame stretch rate for a localised flame surface area, A , as $(1/A)(dA/d\bar{t})$, where \bar{t} is a dimensionless time equal to tu_ℓ^2/ν . This is directly comparable with a similar dimensionless stretch rate, a^* , for an unstable laminar flame.

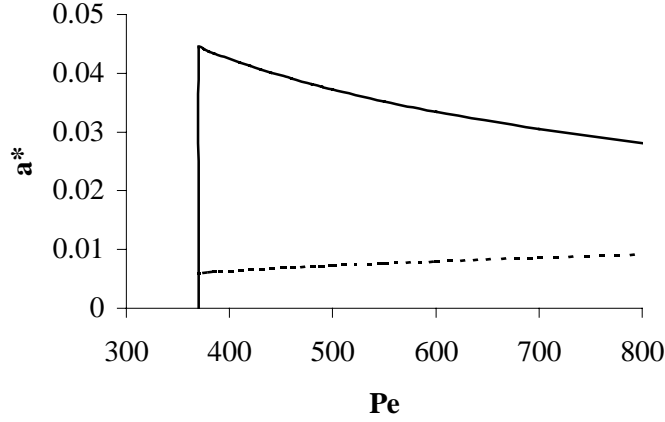


Figure 4. Variation of dimensionless stretch rate, a^* , (full curve) and flame speed (broken curve) due to flame instabilities.

An unstable spherical explosion flame is considered. The ratio of the flame speed, S , arising from surface wrinkling at a mean radius, r , to the laminar flame speed, S_ℓ , of a smooth sphere of the same radius is equal to the ratio of the wrinkled area, A , to the smooth surface area, A_ℓ :

$$A/A_\ell = S/S_\ell, \text{ where } S = dr/dt \quad (16)$$

Somewhat similarly to in Eq. (8), this surface area ratio is equated to the ratio of the area of the fractal surface with the largest unstable wavelength as the outer cut-off to that with the shortest unstable wavelength as the inner cut-off [35].

The mean dimensionless stretch rate of the surface wrinkled by instabilities is $(1/A)(dA/d\bar{t})$. With r normalised by δ_ℓ to give the Peclet number, Pe , and S normalised by u_ℓ , the dimensionless stretch rate, a^* , becomes:

$$a^* = \frac{1}{dPe/d\bar{t}} \frac{d^2Pe}{d\bar{t}^2} + \frac{2}{Pe} \frac{dPe}{d\bar{t}}, \text{ where } \frac{S}{u_\ell} = \frac{dPe}{d\bar{t}} \quad (17)$$

Analysis of the unstable wavelengths as a function of Ma_{sr} , together with the density ratio and Pe , enables A/A_ℓ to be evaluated. The analysis also yields [35,36]:

$$Pe = Pe_o + B\bar{t}^{3/2} \quad (18)$$

which expresses the variation in radius with time after a cellular flame structure has developed at a critical Peclet number, Pe_{cl} . The value of Pe_o is related to Pe_{cl} . The value of \bar{t} is taken to be zero when $Pe = Pe_o$ and the numerical constant, B , depends on Ma_{sr} , the density ratio and stability theory. Some values of B are given in [36].

Equations (17) and (18) give:

$$a^* = \frac{1}{2} \left(\frac{B}{Pe - Pe_o} \right)^{2/3} + \frac{3B^{2/3}}{Pe} (Pe - Pe_o)^{1/3} \quad (19)$$

Shown in Fig. 4 by the full line curve is the variation of a^* with Pe , obtained from Eq. (19), for an unstable flame with $Pe_{cl} = 370$, $Pe_o = 205$ and $B = 0.62$. These values are taken from [36] for a negative value of Ma_{sr} . The broken curve shows $S/u_\ell 10^{-3}$. Even with such an unstable flame, the associated dimensionless stretch factor a^* has a maximum value of less than 0.05, which is relatively small compared with many practical values of K . This is in agreement with the direct numerical simulations of unstable flames by Boughanem and Trouvé [37], who suggested instabilities became important in turbulent combustion only at low values of both Ma and K . However, an increase in pressure for a given distance scale will reduce Pe and Ma_{sr} . The consequent increase in a^* could make it comparable to K . The unique burner measurements by Kobayashi et al. [38] of u_t at pressures of up to 30 atm. appear to confirm the increased importance of instabilities at high pressure.

Conclusions

A number of limitations in the above analyses are apparent. One concerns the derivation and incorporation of accurate data on extinction stretch rates. Another, the legitimacy of using steady state flame stretch and extinction data in unsteady conditions and *vice-versa*. More information is needed about flames subjected to negative flame stretch, the pdf of stretch rates at high Reynolds numbers and the complexities of turbulent flame extinction. In measurements of u_t a distinction should be made between mass burning and entrainment rate burning velocities. Negative values of Ma_{sr} are of interest for two reasons; as revealed by Fig. 2 they may cause enhancement of U , with possible further enhancement by flame instabilities, particularly if K is small. These effects become important in high pressure combustion.

The data on U in Fig. 3 reveal a large spread of values and raise questions as to the importance of flame quenching. Experimentally, flame quenching is observed when $KLe \geq 2.4$ [39], an even more severe quenching than is suggested by Fig. 2.

Although the present study has concentrated on premixtures, much of it is relevant to non-premixed combustion. This is because the mixing between fuel and oxidant can generate stretch rates that no diffusion flamelet can survive. Although there is the added complication of a distribution of equivalence ratios, premixed stretched flamelets combined with Reynolds stress modelling are capable of predicting lift-off heights and blow-off velocities of jet flames [28,40]. Further downstream, the range of possible reactant mixtures is extended and the range of flamelet data required may become prohibitive. The incorporation of reduced reaction schemes [41] into the CFD equations or of JPDF approaches may be preferable. The bulk of the heat release rate occurs in the reaction zone and flamelet modelling of this and u_t is consequently reasonably valid. Reactions that occur beyond the main reaction zone, such as those involving soot formation [42] and thermal NO, cannot be modelled solely by flamelet approaches, although prompt NO can be [11].

References

1. Pope, S. B.: Prog. Energy Combust. Sci., 11, 119 (1985).
2. Saxena, V. and Pope, S. B.: Twenty-Seventh Symposium (International) on Combustion, The Combustion Institute, 1998 p.1081.
3. Peters, N.: Prog. Energy Combust. Sci., 10, 319 (1984).
4. Pitsch, H., Chen, M. and Peters, N.: Twenty-Seventh Symposium (International) on Combustion, The Combustion Institute, 1998 p.1057.
5. Maas, U. and Pope, S. B.: Combust. Flame, 88, 239 (1992).

6. Pope, S. B.: *Combust. Theory Model.*: 1, 1 (1997).
7. Poinso, T., Candel, S. and Trouvé, A.: *Prog. Energy Combust. Sci.*, 21, 531 (1996).
8. Pitsch, H. and Steiner, H.: *Phys. Fluids*, 12, 2541 (2000).
9. Klimenko, A. Y. and Bilger, R. W.: *Prog. Energy Combust. Sci.*, 25, 595 (1999).
10. Poinso, T., Veynante, D. and Candel, S., *Twenty-Third Symposium (International) on Combustion*, Combustion Institute, Pittsburgh, 1991 p.613.
11. Bradley, D., Gaskell, P. H., Gu, X. J., Lawes, M. and Scott, M. J.: *Combust. Flame*, 115, 515 (1998).
12. Bradley, D., Gaskell, P. H. and Gu, X. J.: *Twenty-Seventh Symposium (International) on Combustion*, Combustion Institute, Pittsburgh, 1998 p.849.
13. Bradley, D., Gaskell, P. H. and Gu, X. J.: *Combust. Flame*, 96, 221 (1994).
14. Yeung, P. K., Girimaji, S. S., and Pope, S. B.: *Combust. Flame*, 79, 340 (1990).
15. Bradley, D., Gaskell, P. H. and Gu, X. J.: *Combust. Flame*, 104, 176 (1996).
16. Kolmogorov, A. N., Petrovski, I. G. and Piskonov, N. S.: *Bjul. Moskovkovo Gos. University 1 (7): 1 (1937)*.
17. Zeldovich, Y.: *Combust. Flame* 39, 219 (1980).
18. Libby, P. A.: *Combust. Sci. and Tech.* 68, 15 (1989).
19. Bray, K. N. C.: *Proc. R. Soc. Lond.*, A431, 315 (1900).
20. Bradley, D.: *Twenty - Fourth Symposium (International) on Combustion*, Combustion Institute, 1992 p.247.
21. Bradley, D., Lau, A. K. C. and Lawes, M.: *Phil. Trans. R. Soc. Lond.*, A338, 357 (1992).
22. Gülder, O. L.: *Twenty-Third Symposium (International) on Combustion*, Combustion Institute, 1991 p.835.
23. Bradley, D., Haq, M. Z., Hicks, R. A., Kitagawa, T., Lawes, M., Sheppard, C. G. W. and Woolley, R., in preparation.
24. Trouvé, A. and Poinso, A. J.: *J. Fluid Mech.*, 278, 1 (1994).
25. Duclos, J. M., Veynante, D. and Poinso, T.: *Combust. Flame*, 95,101 (1993).
26. Williams, F. A., "Turbulent combustion", in *The Mathematics of Combustion*, Edited by J.D. Buckmaster, pp. 97-128, SIAM, Philadelphia, 1985.
27. Peters, N.: *J. Fluid Mech.*, 384, 107 (1999).
28. Peters, N.: *Turbulent Combustion*, Cambridge University Press, 2000.
29. Yakhot, V.: *Combust. Sci. and Tech.*, 60, 191 (1988).
30. Ronney, P. D., and Yakhot, V.: *Combust. Sci. and Tech.*, 86, 31 (1992).
31. Sivashinsky, G. I.: *Combust. Sci. and Tech.*, 62, 77 (1988).
32. Klimenko, A. Y.: *Combust. Sci and Tech.*, 139, 15 (1998).
33. Gülder, O. L.: *Twenty-Third Symposium (International) on Combustion*, Combustion Institute, 1991 p.743.
34. Bradley, D., Lawes, M., Scott, M. J. and Mushi, E. M. J.: *Combust. Flame*, 99, 581 (1994).
35. Bradley, D.: *Phil. Trans. R. Soc. Lond.*, 357, 3567 (1999).
36. Bradley, D.: *Combust. Sci. and Tech.*, 158, 15 (2000).
37. Boughanem, H., and Trouvé, A.: *Twenty-Seventh Symposium (International) on Combustion*, Combustion Institute, Pittsburgh 1998, p.971.
38. Kobayashi, H., Kawabata, Y. and Maruta, K.: *Twenty-Seventh Symposium (International) on Combustion*, Combustion Institute, Pittsburgh 1999, p.941.
39. Abdel-Gayed, R. G. and Bradley, D.: *Combust. Flame*, 62, 61 (1985).
40. Bradley, D., Gaskell, P. H. and Gu, X. J.: *Twenty-Seventh Symposium (International) on Combustion*, Combustion Institute, Pittsburgh, 1998 p.1199.
41. Peters, N. and Rogg, B. (Eds.), "*Reduced Kinetic Mechanisms for Applications in Combustion Systems*", Springer-Verlag, Berlin, 1993.
42. Üngüt, A., Bradley, D., Gaskell, P. H. and Gu, X. J.: *Proc. Third Int. Seminar on Fire and Explosion Hazards*, Eds. D. Bradley, D. Drysdale and G. Makhviladze, Uni. Cen. Lancs., 2001 p.436.